Cleveland State University
EngagedScholarship@CSU

Physics Faculty Publications | Physics Department

12-1-1994

Further Thoughts on Newton's Zero-Order Rainbow

James A. Lock
Cleveland State University, j.lock@csuohio.edu

Timothy A. McCollum
Cleveland State University

Follow this and additional works at: https://engagedscholarship.csuohio.edu/sciphysics_facpub

 Part of the Physics Commons

How does access to this work benefit you? Let us know!

Publisher's Statement

Copyright 1994 American Association of Physics Teachers. The article appeared in *American Journal of Physics* 62 (1994): 1082-1089 and may be found at http://aapt.scitation.org/doi/10.1119/1.17665

Original Citation

Lock, James A. and T. A. McCollum. "Further Thoughts on Newton's Zero-Order Rainbow." *American Journal of Physics* 62 (1994): 1082-1089.

Repository Citation

Lock, James A. and McCollum, Timothy A., "Further Thoughts on Newton's Zero-Order Rainbow" (1994). *Physics Faculty Publications*. 25.
https://engagedscholarship.csuohio.edu/sciphysics_facpub/25

This Article is brought to you for free and open access by the Physics Department at EngagedScholarship@CSU. It has been accepted for inclusion in Physics Faculty Publications by an authorized administrator of EngagedScholarship@CSU. For more information, please contact library.es@csuohio.edu.

Further thoughts on Newton's zero-order rainbow

James A. Lock

Timothy A. McCollum

A zero-order rainbow angle may be defined as the relative minimum angle of deviation of geometrical light rays transmitted without internal reflections through a transparent particle. If the incident rays are parallel and the particle is a sphere, such a minimum does not exist. But if the incident rays are not parallel or if the particle has an elliptical rather than circular cross section, an angle of minimum deviation, hence a zero-order rainbow, can occur. For a spherical water droplet, the zero-order rainbow will occur when a point source is placed less than a droplet radius away from its surface. If a column of water with an elliptical cross section is illuminated by a plane wave, a zero-order rainbow will occur if the length of the major axis of the cross section is more than twice the length of the minor axis.

INTRODUCTION

A few years ago there appeared in this journal two commentaries[1,2] on an ambiguous statement in Newton's *Optiks* that was taken to describe either the zero-order rainbow or the 22° ice crystal halo. Independent of what Newton was referring to in the above-mentioned statement, the existence or nonexistence of the zero-order rainbow is an interesting question in its own right. It has long been known that there is no zero-order rainbow associated with the family of initially parallel light rays transmitted through a spherical particle making no internal reflections before exiting.[3] It is the purpose of this article to point out that a zero-order rainbow can occur if either of the above assumptions of (i) parallel incident light rays or (ii) a spherical particle are relaxed.

The organization of this article is as follows. We briefly consider parallel light rays incident on a spherical particle in Sec. II in order to define our notation. In Sec. III we discuss light rays diverging from a point source and incident on a spherical particle. We find that if the point source is closer to the sphere than its paraxial focal point, the deflection angle of the directly transmitted rays as a function of the angle of incidence possesses a relative minimum corresponding to the zero-order rainbow. In Sec. IV we then consider a family of parallel light rays incident on a cylinder with an elliptical cross section. The incident rays are perpendicular to the cylinder axis. We find that if the aspect ratio of the ellipse is such that the rays entering the front surface of the cylinder focus before the center of the cylinder, the deflection angle of the transmitted rays as a function of the angle of incidence again possesses a relative minimum, i.e., the zero-order rainbow. In Sec. V we describe an experiment whose purpose is to observe the zero-order rainbow. Finally, in Sec. VI we present an interpretation of the zero-order rainbow in terms of the spherical aberration caustic far from the conditions for perfect focusing. This interpretation serves to connect two areas of optics (i.e., light scattering and lens aberrations) that one does not usually think of as being related.

PARALLEL LIGHT RAYS INCIDENT ON A SPHERICAL PARTICLE

Consider Fig. 1 where a family of parallel light rays is incident on a spherical particle of radius a and refractive index n. The angle of incidence of a given ray is θ_i, and its transmitted angle θ_t inside the sphere is given by the law of refraction

$$\sin\theta_i = n\sin\theta_t. \tag{1}$$

If the family of rays undergoes $p-1$ internal reflections within the sphere before exiting, the deflection angle θ of the rays with respect to the incident propagation direction is[4]

$$\theta = (p-1)\pi + 2\theta_i - 2p\theta_t. \tag{2}$$

A $p-1$ order rainbow occurs in ray theory at the deflection angle where θ as a function of θ_i possesses a relative minimum,[5]

$$\frac{d\theta}{d\theta_i} = 0 = 1 - \frac{p\cos\theta_i}{n\cos\theta_t}. \tag{3}$$

This may be rewritten using Eq. (1) as

$$\cos\theta_i = \left(\frac{n^2-1}{p^2-1}\right)^{1/2}. \tag{4}$$

The vanishing of the derivative in Eq. (3) at the rainbow deflection angle which we denote by θ^R describes the far-field focusing of the rays. Ray theory also predicts that the light intensity at this angle becomes infinite.[4]

For transmission with no internal reflections ($p=1$), θ is a monotonically increasing function of θ_i and Eq. (4) has no solution. For a spherical particle and parallel incident rays, the zero-order rainbow does not exist.

DIVERGING LIGHT RAYS INCIDENT ON A SPHERICAL PARTICLE

Now consider Fig. 2 where light rays incident on the spherical particle emanate from a point source S a distance $x_s > a$ away from the center of the sphere. The deflection angle with respect to the horizontal axis of the rays making no internal reflections before exiting is now

$$\theta = 2\theta_i - 2\theta_t - \arcsin\left(\frac{a}{x_s}\sin\theta_i\right). \tag{5}$$

Positive values of θ correspond to rays incident on the sphere above the horizontal axis and deflected below the axis or vice versa. Similarly, negative values of θ correspond to rays incident above the horizontal axis and deflected above the

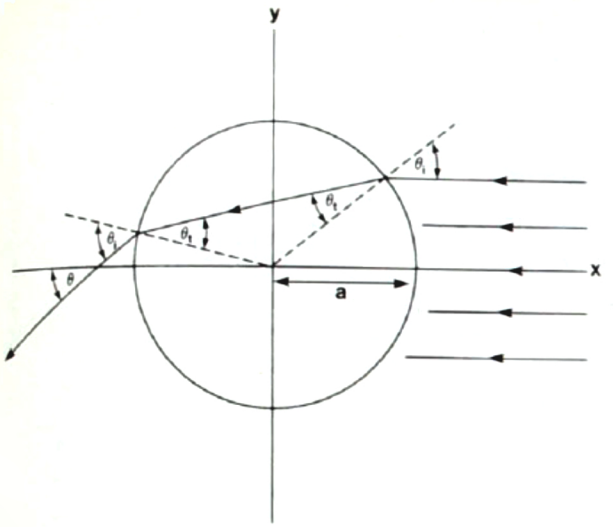

Fig. 1. Trajectory of initially parallel light rays transmitted without internal reflections through a sphere of radius a and refractive index n. The deflection angle of a ray is θ.

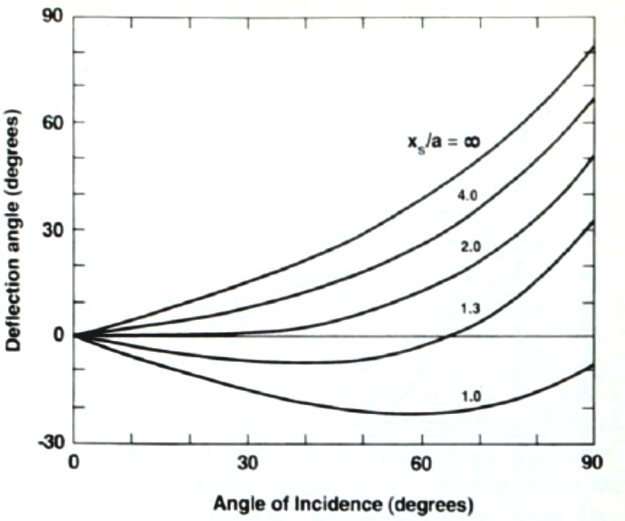

Fig. 3. Deflection angle θ of light rays emanating from a point source and transmitted without internal reflections through a spherical water droplet without internal reflections as a function of the angle of incidence θ_i for a number of values of x_s/a, where a is the droplet radius and x_s is the distance of the point source from the droplet center. For $x_s/a<2.0$, the deflection angle possesses a relative minimum, i.e., a zero-order rainbow.

axis. Figure 3 shows the graph of Eq. (5) for transmission without internal reflections through a water sphere ($n=4/3$) for several values of x_s/a, the distance of the point source from the center of the sphere divided by the sphere radius. For $x_s/a>2.0$, the deflection angle is a monotonically increasing function of θ_i, no zero-order rainbow occurs, and the limit $x_s/a\rightarrow\infty$ corresponds to plane wave incidence as described in Sec. II.

For $x_s/a=2.0$ the deflection angle has its relative minimum at $\theta_i=0$ resulting in strong scattering in the near-forward direction. This is known as a rainbow-enhanced forward glory.[6] The physical reason for its occurrence is as follows. The paraxial focal distance f of a spherical particle is

$$f=\frac{na}{2(n-1)}. \tag{6}$$

For $n=4/3$, approximating a sphere of water, Eq. (6) gives $f=2a$. With $x_s/a=2.0$, strong forward scattering occurs because the point source in Fig. 2 is placed at the sphere's paraxial focal point, and the point source and sphere act in analogy to a search light.[7]

If the point source is closer to the sphere than its focal point, (i.e., $1.0<x_s/a<2.0$), a zero-order rainbow occurs near the forward direction. Since the relative minimum in Fig. 3 is quite broad, many incident light rays participate in the far-field focusing and the zero-order rainbow is expected to be bright. The limit $x_s/a=1.0$ corresponds to a point source on the sphere surface. The zero-order rainbow deflection angle is obtained by solving

$$\frac{d\theta}{d\theta_i}=0=1-\frac{\cos\theta_i}{n\cos\theta_t}-\frac{a}{2x_s}\cos\theta_i\left(1-\frac{a^2}{x_s^2}\sin^2\theta_i\right)^{-1/2} \tag{7}$$

for θ_i and substituting the result into Eq. (5). Equation (7) was solved numerically for several values of x_s/a with $n=4/3$. The resulting deflection angle of the zero-order rainbow is given as a function of x_s/a in Fig. 4. Also shown is the rainbow angle for a glass sphere with $n=1.5$. The results of this section also apply to the cases of a line source parallel to a cylinder of refractive index n and having a circular cross section, and to a point source near the cylinder with observations made in the plane containing the source and perpendicular to the cylinder axis.

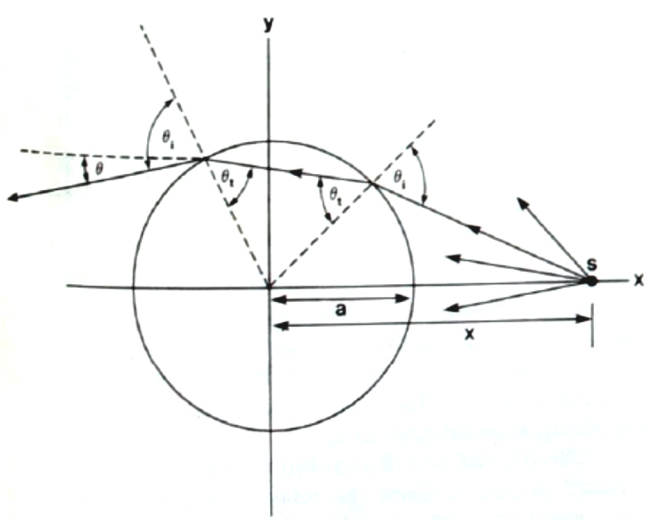

Fig. 2. Trajectory of a light ray emanating from a point source S a distance x_s from the sphere of radius a and refractive index n. The deflection angle of the ray is θ.

PARALLEL LIGHT RAYS INCIDENT ON A CYLINDER WITH AN ELLIPTICAL CROSS SECTION

Since it is possible to produce a zero-order rainbow with a diverging beam incident on a spherical particle, a zero-order

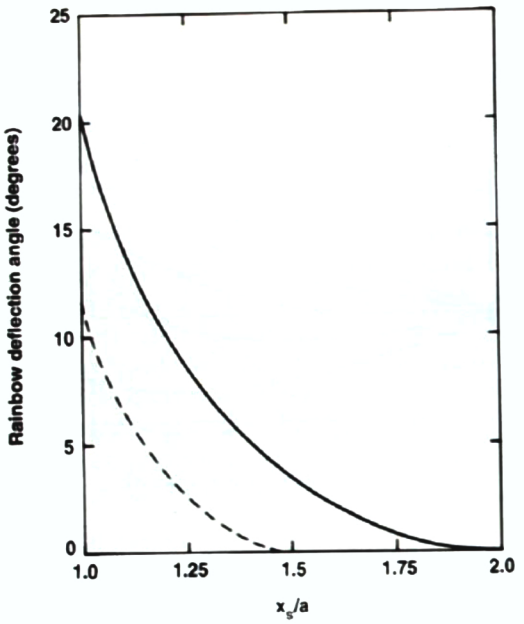

Fig. 4. Deflection angle of the zero-order rainbow θ^R as a function of x_s/a for $n=4/3$ (solid curve) and $n=3/2$ (dashed curve).

rainbow should also occur for parallel illumination of an oblate spheroid. This new geometry is shown in Fig. 5. The structure of rainbows for spheroidal water droplets is complicated, and will be discussed briefly at the end of this section. A simpler case is when a family of parallel light rays is incident on a circular cylinder with an elliptical cross section,[8] a geometry also described by Fig. 5. The equation for the perimeter of the elliptical cross section of the cylinder in rectangular coordinates is

$$\frac{x^2}{b^2}+\frac{y^2}{a^2}=1. \tag{8}$$

Its aspect ratio is b/a, and the radius of curvature R at its leftmost and rightmost ends is a^2/b.

Consider a family of incident light rays parallel to the x axis. A given ray enters the ellipse at the coordinates (x_0,y_0) and exits at the coordinates (x_1,y_1) after traveling a distance

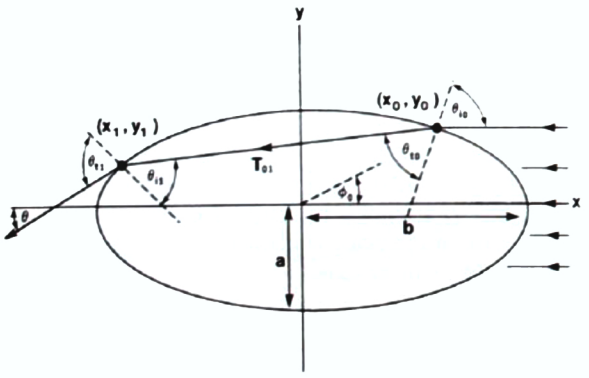

Fig. 5. Trajectory of a light ray through a cylinder whose cross section is of aspect ratio b/a and refractive index n. The distance between the points (x_0,y_0) and (x_1,y_1) is T_{01}. The deflection angle of the ray is θ.

T_{01} inside the ellipse. A combination of much analytic geometry along with the law of refraction gives the following formulas for the various positions, angles, and distances in Fig. 5,

$$\frac{x_0}{a}=\frac{b}{a}\cos\phi_0\left(\cos^2\phi_0+\frac{b^2}{a^2}\sin^2\phi_0\right)^{-1/2}, \tag{9}$$

$$\frac{y_0}{a}=\frac{b}{a}\sin\phi_0\left(\cos^2\phi_0+\frac{b^2}{a^2}\sin^2\phi_0\right)^{-1/2}, \tag{10}$$

$$\tan\theta_{i0}=\frac{b^2}{a^2}\tan\phi_0, \tag{11}$$

$$n\sin\theta_{t0}=\sin\theta_{i0}, \tag{12}$$

$$\frac{T_{01}}{a}=\frac{2\left(\frac{x_0}{a}\cos(\theta_{i0}-\theta_{t0})+\frac{b^2y_0}{a^2a}\sin(\theta_{i0}-\theta_{t0})\right)}{\cos^2(\theta_{i0}-\theta_{t0})+\frac{b^2}{a^2}\sin^2(\theta_{i0}-\theta_{t0})}, \tag{13}$$

$$\frac{x_1}{a}=\frac{x_0}{a}-\frac{T_{01}}{a}\cos(\theta_{i0}-\theta_{t0}), \tag{14}$$

$$\frac{y_1}{a}=\frac{y_0}{a}-\frac{T_{01}}{a}\sin(\theta_{i0}-\theta_{t0}), \tag{15}$$

$$\theta_{i1}=-\arctan\left(\frac{b^2}{a^2}\frac{y_1}{x_1}\right)+\theta_{i0}-\theta_{t0}, \tag{16}$$

and

$$\sin\theta_{t1}=n\sin\theta_{i1}. \tag{17}$$

The deflection angle

$$\theta=\theta_{t1}-\theta_{i1}+\theta_{i0}-\theta_{t0} \tag{18}$$

with respect to the direction of the incident rays was computed as a function of ϕ_0 for a number of values of b/a for a cylinder of water with $n=4/3$. The results are shown in Fig. 6. For $1\leq b/a<2$, the deflection angle is a monotonically increasing function of ϕ_0, no zero-order rainbow occurs, and the limit $b/a=1$ corresponds to a cylinder with circular cross section as in Fig. 1.

For $b/a=2$, the deflection angle has a relative minimum at $\phi_0=0$ and again results in strong scattering in the near-forward direction. The physical reason for this is related to the mechanism described in Sec. III. The paraxial focal length f of a surface with radius of curvature R is

$$f=\frac{nR}{n-1}. \tag{19}$$

For $n=4/3$ and $b/a=2$, we have $R=a/2$ and Eq. (19) gives $f=2a$. The incident paraxial light rays are focused to the center of the cylinder by its front surface. The center is also the focal point of the rear surface. The paraxial rays thus both enter and exit the cylinder parallel to the x axis producing strong forward scattering.

If $2.0<b/a\leq 2.412$, a zero-order rainbow occurs near the forward direction. Since the relative minimum of Fig. 6 is quite sharp in contrast to Fig. 3, only a few incident light rays participate in the far-field focusing, and the zero-order rainbow is expected to be dim. For $b/a>2.412$ a relative minimum in the deflection angle is prevented from occurring by total internal reflection of the light rays at (x_1,y_1). The

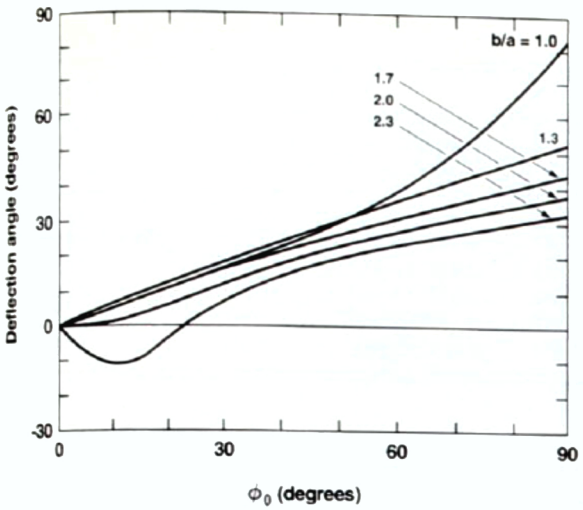

Fig. 6. Deflection angle of initially parallel light rays transmitted without internal reflections through a cylinder of water with an elliptical cross section as a function of the polar coordinate angle ϕ_0 of Fig. 5 and Eqs. (9) and (10) for a number of values of the aspect ratio. The deflection angle possesses a relative minimum, i.e., a zero-order rainbow, for $b/a>2.0$.

deflection angle of the zero-order rainbow as a function of b/a with $n=4/3$ is given in Fig. 7. These results also describe the case of a prolate spheroid whose symmetry axis coincides with the direction of propagation of the plane wave.

The structure of the zero-order rainbow for a family of parallel light rays incident on an oblate spheroid whose surface is given by

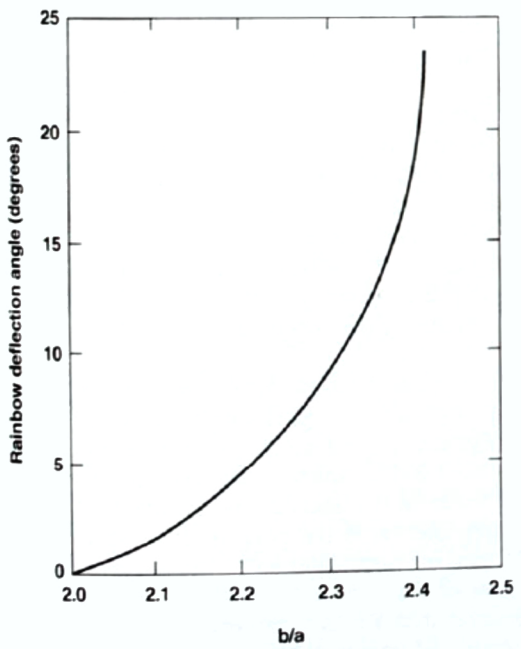

Fig. 7. Deflection angle of the zero-order rainbow of Fig. 6 as a function of the aspect ratio b/a. Total internal reflection prevents the occurrence of the zero-order rainbow for $b/a>2.412$.

$$\frac{x^2}{b^2}+\frac{y^2}{b^2}+\frac{z^2}{a^2}=1 \tag{20}$$

is complicated. First for $b/a>2$, rays incident in the xz plane encounter an elliptical cross section of the spheroid and produce the zero-order rainbow of Fig. 7 in the xz plane. But rays in the xy plane encounter a circular cross section of radius b and produce no zero-order rainbow in the xy plane. Thus the zero-order rainbow does not have circular symmetry about the x axis as was the case for both the usual spherical particle rainbows ($p\geq 2$) of Sec. II and the spherical particle zero-order rainbow of Sec. III. Also, for the first-order rainbow, certain rays not incident in the xz plane, called skew rays, have trajectories through the spheroid that cause them to exit parallel to the xz plane and participate along with the rays incident in the xz plane in far-field rainbow formation.[9,10] These multiray rainbows correspond to higher order scattering caustics[11] and presumably occur for the zero-order rainbow as well.

Freely falling raindrops become oblate due to air resistance, and the degree of oblateness increases with increasing droplet size. But for realistic size droplets with radii of the order of a few millimeters,[12] $b/a\lesssim 1.4$ which is far below the value required to produce a zero-order rainbow during a rain shower.

OBSERVATION OF THE ZERO-ORDER RAINBOW FOR DIVERGING LIGHT RAYS INCIDENT ON A WATER-FILLED SPHERICAL GLOBE

A spherical thin-walled glass globe of outer radius $a=95.25\pm0.25$ mm and glass thickness of approximately 0.75 mm was filled with water. The light incident on the globe was provided by a 200 W Sylvania Clear Utility Light. The filament of the lightbulb is suspended vertically by the manufacturer within the bulb's clear glass envelope at a distance of 32.75 ± 0.50 mm from its outer surface. The diameter of the filament was measured to be 1.59 ± 0.02 mm by imaging it through a lens onto a distant viewing screen. When the lightbulb is placed so that the midpoint of the filament is in the equatorial plane of the globe, the filament acts as an approximate point source for scattering in the horizontal plane.

The light transmitted through the globe in the near-forward direction was observed on a wall 11.19 ± 0.005 m away from the center of the globe. When the distance x_s between the filament and the center of the globe was greater than approximately 200 mm, the near-forward transmitted light was diffuse [Fig. 8(a)]. But when the lightbulb was moved closer to the globe so that $x_s=198.0\pm0.5$ mm, a slightly misfocused image of the filament appeared on the wall [Fig. 8(b)]. When the lightbulb was moved closer to the globe, the image first became increasingly misfocused, and then evolved into a nearly uniformly bright white region a few degrees wide with distinctly reddish boundaries [Fig. 8(c)]. Outside these boundaries, the transmitted light was quite dim. The angle with respect to the forward direction of the reddish boundaries increased as the lightbulb was moved closer to the globe. Our claim is that this distinctly reddish boundary between the bright and dim regions is the zero-order rainbow. Its reddish color is due to the fact that the rainbow angle for red light is larger than that for blue light. Thus the extremum deflection angle for blue light corre-

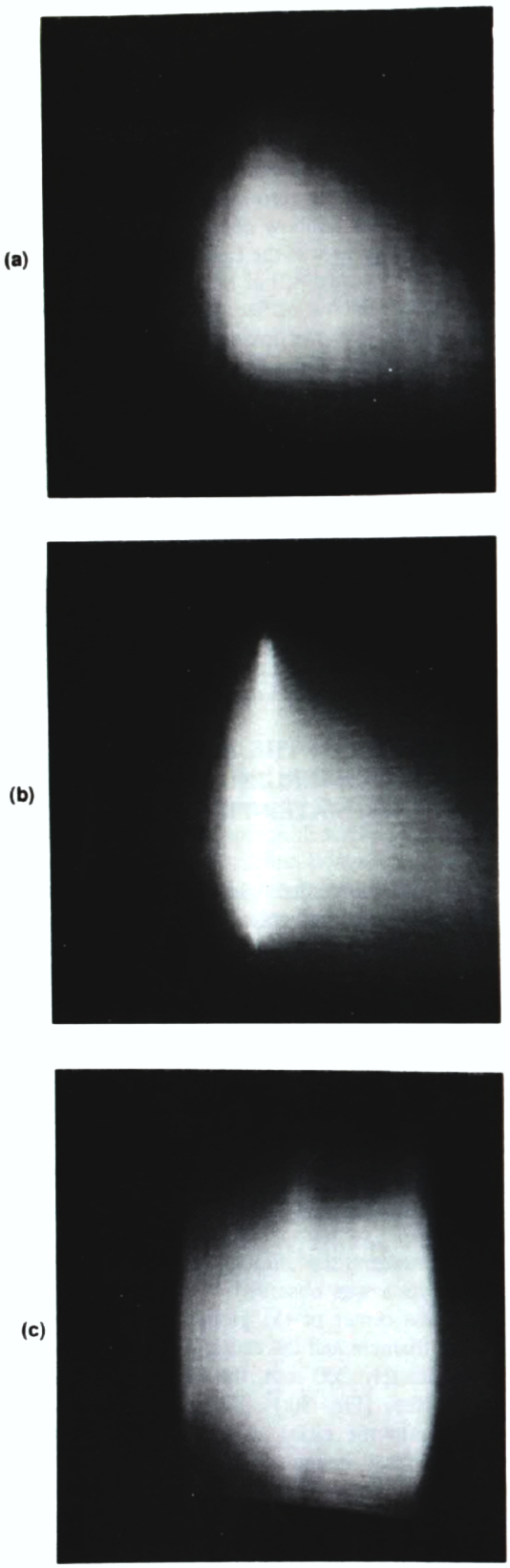

Fig. 8. Transmitted light intensity in the near-forward direction for (a) $x_s/a > 2.0$. The transmitted light is rather diffuse. (b) $x_s/a \approx 2.0$. A misfocused image of the source appears on the viewing screen. (c) $x_s/a < 2.0$. The zero-order rainbow is evident with an illuminated region at smaller deflection angles and an unilluminated region at larger deflection angles.

Table I. Experimental and theoretical deflection angle of the zero-order rainbow.

Ratio of source dist. to radius x_s/a	Rainbow deflection angle (experimental)	Rainbow deflection angle [from Eqs. (5) and (7)]	Rainbow deflection angle [with corrections to Eqs. (5) and (7)]
1.8741	0.555°±0.027°	0.356°	0.510°
1.7637	1.248°±0.037°	0.952°	1.159°
1.6745	2.021°±0.037°	1.632°	1.875°
1.5642	3.035°±0.043°	2.761°	3.045°
1.4541	4.547°±0.057°	4.286°	4.610°
1.3439	6.687°±0.084°	6.348°	6.714°

sponds to a transmitted angle for all other colors, producing a net white color assuming a white light source. The extremum deflection angle for red light is beyond the range of transmitted angles for all other colors, producing the reddish boundary.[13] The bright white region observed at smaller deflection angles is analogous to the supernumerary region for the first-order rainbow, and the dim region at larger deflection angles is analogous to Alexander's dark band.

The angle with respect to the forward direction of the zero-order rainbow was measured as a function of x_s/a and is shown in the second column of Table I. The rainbow deflection angle in each case has been corrected for the width of the filament. This correction was made in the following way. The shape of the lightbulb filament is a helix. When the image of the filament was observed on the distant viewing screen, the vertical center line of the image appeared continuous due to the forward portions of the helix crossing in front of the rear portions. The left and right vertical edges of the image, however, contained gaps between the locations where the helix turned back on itself. As a result, the brightness profile of the filament, averaged in the vertical direction, is not uniform. It is brightest along the vertical center line, with the brightness falling off near the filament's left and right edges. Thus the effective width of our light source is smaller than the diameter of the filament. Curve fitting the shape of the image of the helical coil and integrating over it, we calculated the root-mean-square diameter of the filament to be 0.76 mm. We used this rms filament diameter in the finite source width correction. The correction decreased with experimental rainbow scattering angle by 0.122° for $x_s/a = 1.8741$, and by 0.168° for $x_s/a = 1.3439$ at which point the clear glass envelope of the lightbulb and the globe were in contact. The uncertainty in the measured scattering angles in Table I is due to the observed width of the reddish boundary.

The theoretical rainbow deflection angle was calculated using Eqs. (5) and (7) and is shown in the third column of Table I. The index of refraction of the water in the globe was taken to be 1.3316, which is the average of the refractive index of water in the interval[14] $0.59\ \mu m \leq \lambda \leq 0.70\ \mu m$. This wavelength interval is the portion of the spectrum locus in the *CIE* chromaticity diagram[15,16] that visually appears red. The results of Eqs. (5) and (7) follow the same trend as the experimental data for the zero-order rainbow. But they are consistently and unacceptably too low, by about 0.29° on the average.

In order to account for the errors resulting from the departures of our experimental setup from the assumptions of Sec. III, two theoretical corrections were made, the details of

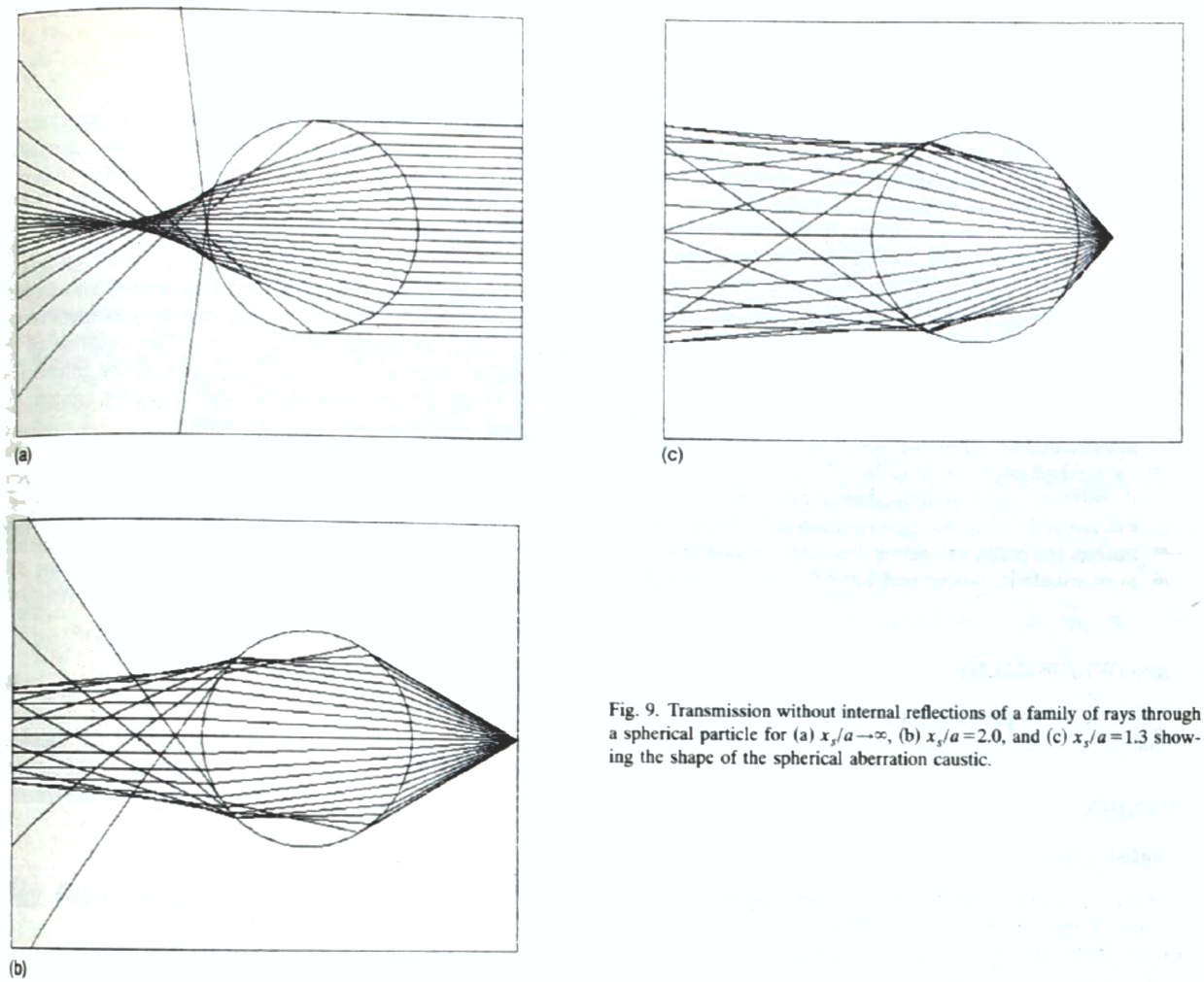

Fig. 9. Transmission without internal reflections of a family of rays through a spherical particle for (a) $x_s/a \to \infty$, (b) $x_s/a = 2.0$, and (c) $x_s/a = 1.3$ showing the shape of the spherical aberration caustic.

which appear in the Appendix. The first correction takes into account the thickness of the glass wall of the globe. Assuming a thickness of 0.75 mm and a refractive index of 1.5 for the glass, this correction increases the theoretical rainbow deflection angle[17] by 0.021° for $x_s/a = 1.8741$, and by 0.064° for $x_s/a = 1.3439$. Although this pushes the theoretical results in the right direction, the increase is not nearly enough to match the experimental data. On the other hand, the small size of the correction justifies the use of only an approximate thickness and refractive index for the glass.

The second correction takes into account the fact that the viewing screen is 117.5 ± 0.05 globe radii from the center of the globe rather than being infinitely far away as assumed by Eqs. (5) and (7). The location of the zero-order rainbow caustic was analytically calculated as a function of distance from the center of the globe.[18] The caustic bends somewhat as it leaves the globe surface and becomes asymptotic to the rainbow deflection angle θ^R far from the globe. Thus at the viewing screen, the measured deflection angle θ_{caustic} differs somewhat from θ^R. This viewing screen location correction increases the theoretical deflection angle by 0.134° for $x_s/a = 1.8741$, and by 0.302° for $x_s/a = 1.3439$. These two corrections added to the results of Eqs. (5) and (7) are the corrected theoretical results shown in the last column of Table I. The comparison between the corrected theoretical results and experiment is now excellent, the difference between the two being about 0.06° on the average. Thus we are confident that the distinctly reddish region we have observed is the zero-order rainbow.

Similar experiments could be performed using a large glass sphere. The zero-order rainbow, however, would be more difficult to observe. This is because, as is shown in Fig. 4, the light source must be placed closer to the glass sphere than it is to the water-filled globe, and the rainbow occurs at a smaller deflection angle.

THE ZERO-ORDER RAINBOW AS A SPHERICAL ABERRATION CAUSTIC

The two surfaces of a spherical lens are segments of spheres. A spherical particle is thus a special case of a thick spherical lens. In the usual theory of thin spherical lenses, if the incident and refracted angles of the paraxial rays are approximated by the first term of their Taylor series expansions, all the transmitted paraxial rays leaving a point source on the optical axis pass through a single image point producing perfect focusing. In actuality however, the edge rays focus closer to the lens than do the paraxial rays, producing the cusp-shaped spherical aberration caustic whose apex is the paraxial image position.[19,20] This is shown in Fig. 9(a) for

initially parallel rays transmitted through a spherical particle. As the point source on the axis approaches the right paraxial focal point as in Fig. 9(b), the apex of the spherical aberration caustic moves off to infinity. In terms of elementary lens theory, this corresponds to the image point also moving off to infinity. If the point source is then moved through the paraxial focal point, the two branches of the spherical aberration caustic no longer converge to form an apex. They diverge instead. This is shown in Fig. 9(c). These two diverging branches of the spherical aberration caustic are the zero-order rainbow of Sec. III. This phenomenon is not peculiar to spherical particles, but occurs for all coverging spherical lenses. In the language of lens aberrations, the color of the zero-order rainbow is due to the transverse chromatic aberration of the spherical aberration caustic.[19,20]

The zero-order rainbow, although appearing novel or exotic when considered from the point of view of scattering theory, is an extension of familiar ideas when considered from the point of view of lens aberrations. This extension consists of not only considering lens aberration caustics near the conditions for perfect imaging, but also considering their remnants in situations where real image formation is impossible.

ACKNOWLEDGMENT

This work was supported in part by the National Aeronautics and Space Administration Grant No. NCC3-204.

APPENDIX

Coated sphere

Consider a coated sphere whose core has radius a and refractive index n_1, and whose coating has thickness δ and refractive index n_2. The angle of incidence of a light ray at the air-coating interface is θ_3, and its angle of refraction in the coating is θ_2. The angle of incidence of the ray at the coating-core interface is θ_2', and its angle of refraction in the core is θ_1. These angles are related to each other by

$$\sin\theta_3 = n_2 \sin\theta_2, \tag{A1}$$

$$\frac{\sin\theta_2}{a} = \frac{\sin\theta_2'}{a+\delta}, \tag{A2}$$

and

$$n_2 \sin\theta_2' = n_1 \sin\theta_1. \tag{A3}$$

If a family of parallel light rays is incident on the coated sphere, its paraxial focal point is

$$f = \frac{(a+\delta)}{2}\frac{n_1}{(n_1-1)}\left[1+\frac{\delta}{a}\left(\frac{n_2-n_1}{n_1-1}\right)\frac{1}{n_2}+\theta\left(\frac{\delta^2}{a^2}\right)\right]. \tag{A4}$$

If light rays emanating from a point source S a distance x_s from the center of the coated sphere are incident on it, the deflection angle of a transmitted ray is

$$\theta = 2\theta_3 + 2\theta_2' - 2\theta_2 - 2\theta_1 - \arcsin\left(\frac{a+\delta}{x_s}\sin\theta_3\right). \tag{A5}$$

The deflection angle of the zero-order rainbow is obtained by numerically solving

$$\frac{d\theta}{d\theta_3} = 0 \tag{A6}$$

for θ_3 and substituting the result into Eq. (A5).

Finite screen distance

For a homogeneous sphere of radius a, the equation of a transmitted ray in rectangular coordinates after it has exited the sphere is

$$y = -\tan\theta\, x + \frac{a\sin\theta_i}{\cos\theta}, \tag{A7}$$

where θ is the deflection angle of the ray and θ_i is its angle of incidence on the sphere. Consider two rays incident on the sphere with the angles θ_i and $\theta_i+\epsilon$. The equation of the zero-order rainbow caustic is the locus of the intersection points of the exiting rays in the limit $\epsilon\to 0$ for arbitrary θ_i. Carrying out this procedure we obtain

$$\begin{aligned}\frac{x}{a} &= \frac{1}{\Delta}(\cos\theta_i\cos\theta + \Delta\sin\theta_i\sin\theta),\\ \frac{y}{a} &= \frac{1}{\Delta}(\cos\theta_i\sin\theta - \Delta\sin\theta_i\cos\theta),\end{aligned} \tag{A8}$$

where

$$\Delta = 2 - \frac{2\cos\theta_i}{n\cos\theta_t} - \frac{a}{x_s}\cos\theta_i\left(1-\frac{a^2}{x_s^2}\sin^2\theta_i\right)^{-1/2}. \tag{A9}$$

As was seen in Eq. (7), the far-field limit of the caustic is obtained when $\Delta\to 0$. The deflection angle θ_{caustic} of the zero-order rainbow at a distance x from the center of the sphere is given by

$$\tan\theta_{\text{caustic}} = \frac{y}{x}. \tag{A10}$$

Combined formulas

If the light rays are incident on a coated sphere rather than a homogeneous sphere, the equation of the zero-order rainbow caustic becomes

$$\begin{aligned}\frac{x}{a+\delta} &= \frac{1}{\Delta_c}(\cos\theta_3\cos\theta + \Delta_c\sin\theta_3\sin\theta),\\ \frac{y}{a+\delta} &= \frac{1}{\Delta_c}(\cos\theta_3\sin\theta - \Delta_c\sin\theta_3\cos\theta),\end{aligned} \tag{A11}$$

where

$$\begin{aligned}\Delta_c = 2 &- \frac{2}{n_1}\left(\frac{a+\delta}{a}\right)\frac{\cos\theta_3}{\cos\theta_1} - \left(\frac{a+\delta}{x_s}\right)\\ &\times\cos\theta_3\left[1-\left(\frac{a+\delta}{x_s}\right)^2\sin^2\theta_3\right]^{-1/2}\\ &+ \frac{2}{n_2}\left(\frac{a+\delta}{a}\right)\frac{\cos\theta_3}{\cos\theta_2'} - \frac{2}{n_2}\frac{\cos\theta_3}{\cos\theta_2}.\end{aligned} \tag{A12}$$

The deflection angle of the zero-order rainbow a distance x from the center of the sphere is again given by Eq. (A10).

[a]Present address: Physics Department, University of North Carolina, Chapel Hill, North Carolina 27599.

[1]C. F. Bohren and A. B. Fraser, "Newton's zero-order rainbow: Unobservable or nonexistent?," Am. J. Phys. **59**, 325–326 (1991).

[2]A. E. Shapiro, "Comment on 'Newton's zero-order rainbow: Unobservable or nonexistent?,'" Am. J. Phys. **60**, 749–750 (1992).

[3]W. J. Humphreys, *Physics of the Air* (Dover, New York, 1964), p. 500.
[4]J. D. Walker, "Multiple rainbows from single drops of water and other liquids," Am. J. Phys. **44**, 421–433 (1976).
[5]H. M. Nussenzveig, "The theory of the rainbow," Sci. Am. **236**(4), 116–127 (1977).
[6]D. S. Langley and M. J. Morrell, "Rainbow-enhanced forward and backward glory scattering," Appl. Opt. **30**, 3459–3467 (1991).
[7]The analogous situation of exceptionally strong scattering at 180° for $p=2$ and $n=2$ is described in P. L. Marston, "Geometrical and catastrophe optics methods in scattering," Phys. Acous. **21**, 1–234 (1992), Sec. 4.8; and in J. F. Nye, "Rainbows from ellipsoidal water drops," Proc. R. Soc. London, Ser. A **438**, 397–417 (1992).
[8]This is related to the case of parallel light rays incident on a column of water with a circular cross section which was experimentally examined by F. Billet in the 19th century. His results are summarized in C. B. Boyer, *The Rainbow from Myth to Mathematics* (Princeton University Press, Princeton, NJ, 1987), p. 309. The effect of water droplet ellipticity on the first order rainbow was first calculated by W. Möbius "Zur Theorie des Regenboges und ihren experimentallen Prüfung," Abh. Wiss. Kgl. Ges. Sächs, Math. Phys. Kl. **30**, 108–254 (1907). His results are summarized and extended in A. B. Fraser, "Why can the supernumerary bows be seen in a rain shower?," J. Opt. Soc. Am. **73**, 1626–1628 (1983), and in G. P. Können, "Appearance of supernumeraries of the secondary rainbow in rain showers," *ibid.* **A4**, 810–816 (1987).
[9]P. L. Marston and E. H. Trinh, "Hyperbolic umbilic diffraction catastrophe and rainbow scattering from spheroidal drops," Nature **312**, 529–531 (1984).
[10]J. F. Nye, "Rainbow scattering from spheroidal drops—an explanation of the hyperbolic umbilic foci," Nature **312**, 531–532 (1984).
[11]M. V. Berry and C. Upstill, "Catastrophe optics: Morphologies of caustics and their diffraction patterns," Prog. Opt. **18**, 257–346 (1980).
[12]A. W. Green, "An approximation for the shapes of large raindrops," J. Appl. Meteorol. **14**, 1578–1583 (1975). Even for acoustically levitated droplets, it is difficult to maintain droplet stability for $b/a \gtrsim 1.7$. See, for example, the caption of Fig. 2 of this reference and also G. Kaduchak, P. L. Marston, and H. J. Simpson, "E_6 diffraction catastrophe of the primary rainbow of oblate water drops: Observations with white light and laser illumination," Appl. Opt. **33**, 4691–4696, 4961 (1994).
[13]The reddish boundary also occurs for sun dogs produced by transmission without internal reflections of sunlight through ice crystals in the atmosphere. See, for example, R. Greenler, *Rainbows, Halos, and Glories* (Cambridge University Press, New York, 1980) p. 28.
[14]J. K. Robertson, *Introduction to Optics, Geometrical and Physical*, 4th ed. (Van Nostrand, Princeton, NJ, 1954), p. 102, Table 3.
[15]D. Falk, D. Brill, and D. Stork, *Seeing the Light* (Harper and Row, New York, 1986), Color plate 9.2.
[16]R. C. Gonzalez and P. Wintz, *Digital Image Processing* (Addison–Wesley, Reading, MA, 1977), Color plate IV.
[17]J. A. Lock, J. M. Jamison, and C.-Y. Lin, "Rainbow scattering by a coated sphere," Appl. Opt. **33**, 4677–4690, 4960 (1994).
[18]J. A. Lock and E. A. Hovenac, "Internal caustic structure of illuminated liquid droplets," J. Opt. Soc. Am. **A8**, 1541–1552 (1991), Appendix A.
[19]F. A. Jenkins and H. E. White, *Fundamentals of Optics*, 3rd ed. (McGraw–Hill, New York, 1957), Chap. 9.
[20]E. Hecht, *Optics*, 2nd ed. (Addison–Wesley, Reading, MA, 1987), Sec. 6.3.

Post-print standardized by MSL Academic Endeavors, the imprints of the Michael Schwartz Library at Cleveland State University, 2017.